New Zn 2+ Metal Organic Frameworks with Unique Network Topologies from the Combination of Trimesic Acid and Amino- Alcohols

ARTICLE *in* CRYSTAL GROWTH & DESIGN · NOVEMBER 2012

Impact Factor: 4.89 · DOI: 10.1021/cg301047w

4 AUTHORS:

Manolis J Manos
University of Ioannina
94 PUBLICATIONS **1,232** CITATIONS
SEE PROFILE

Eleni Moushi
University of Cyprus
38 PUBLICATIONS **613** CITATIONS
SEE PROFILE

Giannis S. Papaefstathiou
National and Kapodistrian University of Athens
97 PUBLICATIONS **2,586** CITATIONS
SEE PROFILE

Anastasios J Tasiopoulos
University of Cyprus
128 PUBLICATIONS **2,813** CITATIONS
SEE PROFILE

CRYSTAL GROWTH & DESIGN

Article

pubs.acs.org/crystal

New Zn^{2+} Metal Organic Frameworks with Unique Network Topologies from the Combination of Trimesic Acid and Amino-Alcohols

Manolis J. Manos,[†] Eleni E. Moushi,[†] Giannis S. Papaefstathiou,*[,‡] and Anastasios J. Tasiopoulos*[,†]

[†]Department of Chemistry, University of Cyprus, 1678 Nicosia, Cyprus

[‡]Laboratory of Inorganic Chemistry, Department of Chemistry, National and Kapodistrian University of Athens, Panepistimiopolis, Zografou 157 71, Athens, Greece

Supporting Information

ABSTRACT: A series of new Zn^{2+}-trimesate (btc^{3-}) metal organic frameworks (MOFs) has been isolated in the presence of various amino-alcohols under solvothermal conditions. Thus, the reaction of $ZnCl_2$ with trimesic acid (H_3btc) and the amino-alcohols triethanolamine (teoa), 2-(hydroxymethyl)piperidine (hmpip), *N*-*tert*-butyldiethanolamine (tbdeoa), 1,4-bis(2-hydroxyethyl)piperazine (bhep), *N*-methyldiethanolamine (mdeoa), or 4-(2-hydroxyethyl)-morpholine (hem) in a 1.6:1:5.6 molar ratio in DMF afforded compounds $(teoaH)_2[Zn(btc)_{1.33}]$ (**MOAAF-1**) (MOAAF = metal organic amino-alcohol framework), $(NH_2Me_2)_2(hmpipH)[Zn_3(btc)_3]$ (**MOAAF-2**), $(NH_2Me_2)(tbdmaH)_2[Zn_3(btc)_3]$ (**MOAAF-3**) (tbdma = *N*-*tert*-butyldimethylamine), $(NH_2Me_2)(bhepH_2)[Zn_3(btc)_3]$ (**MOAAF-4**), $(NH_2Me_2)[Zn_4(btc)_3(mdeoa)_2]$ (**MOAAF-5**), and $(NH_2Me_2)[Zn_4(btc)_3(hem)_2]$ (**MOAAF-6**), respectively. The compounds display 3D structures with relatively large cavities (4−10 Å) and high potential solvent-accessible areas (38−68% of the unit cell volumes). A number of novel structural features are revealed in the reported MOFs, such as unprecedented dinuclear $[Zn_2(COO)_5]^{-1}$ secondary building units (SBUs) and unique network topologies (e.g., in compounds **MOAAF-2**, **MOAAF-3**, **MOAAF-5**, and **MOAAF-6**). The amino-alcohols employed played a key role for the appearance of such novel structural features in **MOAAF 1−6** since they were found to act as bases responsible for the deprotonation of H_3btc, templates, and chelating ligands. Specifically, most of the compounds synthesized were shown to be templated by protonated amino-alcohols that are involved in hydrogen bonding interactions with the frameworks, whereas in two cases (compounds **MOAAF-5** and **MOAAF-6**) the amino-alcohols acted as chelating ligands affecting significantly the underline topology of the MOFs. The thermal stability and photoluminescence properties of the MOFs are also discussed. This work represents the initial systematic investigation on the use of combination of amino-alcohols and polycarboxylate ligands for the synthesis of new MOFs, demonstrating it as a powerful synthetic strategy for the isolation of novel MOFs.

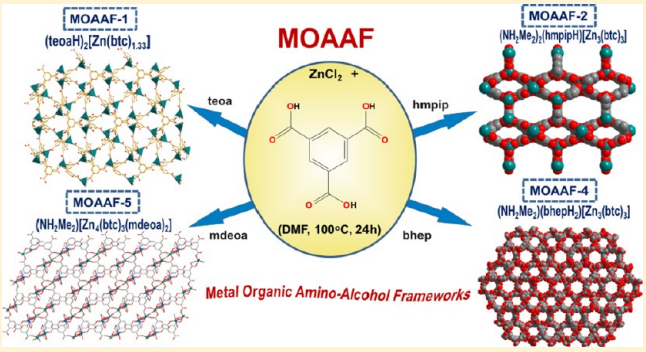

INTRODUCTION

The tremendous interest in metal organic frameworks (MOFs) over the past decade is due not only to their aesthetically pleasing structures and unique structural topologies[1−4] but also to their potential applications in many areas including catalysis,[5] magnetism,[6] gas storage,[7−11] sensing, etc.[12] The key factor for the discovery of MOFs with novel structural features and potentially interesting physical properties is the development of new synthetic strategies. It is widely known that the employment of templates is a successful approach toward new porous materials.[13] Concerning the templated synthesis of MOFs, there have been several reports on the use of various structure-directing agents such as amines,[14] alcohols,[15] alkali ions,[16] polyoxometalates,[17] metal complexes,[18] surfactants,[19a] urea derivatives,[19b] etc. Thus, a plethora of new MOFs have been isolated with many of them showing unprecedented structural characteristics and in some cases guest-induced properties such as enhancement of porosity,[20] electrochemical properties,[21] catalytic activity,[22] etc. Although a number of organic compounds have been tested as templates in the synthesis of new MOFs, amino-alcohols have received much less attention.[23] This is rather surprising, since amino-alcohols may accomplish a variety of functions to facilitate the formation of new structures including deprotonation of the oxygen atoms of the polytopic organic ligands (e.g., carboxylic), templating effect, as well as ligation to the metal ions. In particular, these organic molecules may be highly efficient as structure-directing agents due to their excellent capability for formation of

Received: July 23, 2012
Revised: September 12, 2012
Published: September 18, 2012

hydrogen bonds. Furthermore, they can be quite effective as ligands for the metal ions displaying a variety of coordination modes, such as terminal, chelating, or bridging ligation, resulting often in the assembly of high nuclearity metal clusters.[24−31] Thus, amino-alcohols could lead to MOFs with new structural types not only due to their strong templating effect but also because they are powerful ligands that may stabilize unprecedented secondary building units (SBUs).

Recently, we have initiated a research program that involves the use of a combination of polytopic organic ligands typically leading to polymeric structures and various amino-alcohols that can act either as structure-directing agents or ligands for the synthesis of new MOFs. Herein we present the first results of these investigations, compounds $(teoaH)_2[Zn(btc)_{1.33}]$ (**MOAAF-1**) (**MOAAF** = metal organic amino-alcohol framework), $(NH_2Me_2)_2(hmpipH)[Zn_3(btc)_3]$ (**MOAAF-2**), $(NH_2Me_2)(tbdmaH)_2[Zn_3(btc)_3]$ (**MOAAF-3**) (tbdma= *N-tert*-butyl-dimethylamine), $(NH_2Me_2)(bhepH_2)[Zn_3(btc)_3]$ (**MOAAF-4**), $(NH_2Me_2)[Zn_4(btc)_3(mdeoa)_2]$ (**MOAAF-5**), and $(NH_2Me_2)[Zn_4(btc)_3(hem)_2]$ (**MOAAF-6**), which have been isolated by combining trimesic acid (H_3btc) and triethanolamine (teoa), 2-(hydroxymethyl)piperidine (hmpip), *N-tert*-butyldiethanolamine (tbdeoa), 1,4-bis(2-hydroxyethyl)-piperazine (bhep), *N*-methyldiethanolamine (mdeoa), or 4-(2-hydroxyethyl)morpholine (hem) (Scheme 1). Although the structures of these new MOFs are based on the same polytopic ligand, they exhibit a remarkable diversity and unique structural−topological features that are clearly induced by the various amino-alcohols. The thermal stability and photoluminescence properties of the compounds are also reported. To the best of our knowledge, this study represents the initial systematic investigation on the use of a combination of polytopic ligands and amino − alcohols for the synthesis of novel MOFs.

Scheme 1. Amino-Alcohols Employed in This Study

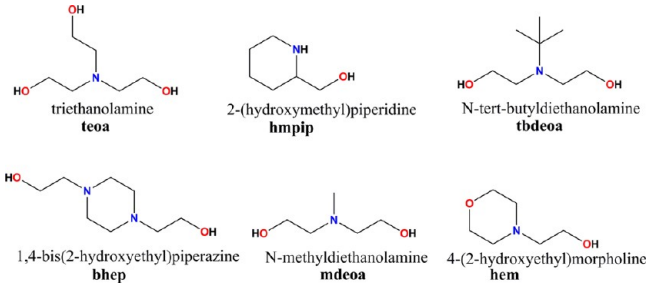

EXPERIMENTAL SECTION

Materials. All procedures were performed under aerobic conditions. Solvents and reagents were obtained from commercial sources and used as received.

Physical Measurements. Elemental analyses (C, H, N) were performed by the in-house facilities of the University of Cyprus, Chemistry Department. IR spectra were recorded on KBr pellets in the 4000−400 cm^{-1} range using a Shimadzu Prestige-21 spectrometer. PXRD diffraction patterns were recorded on a Shimazdu 6000 Series X-ray diffractometer (Cu Kα radiation, λ = 1.5418 Å). Photoluminescence (PL) spectra were obtained on an Edinburgh Xe900 spectrofluorometer. Thermal stability studies were performed with a Shimadzu TGA 50 thermogravimetric analyzer.

Syntheses. ***MOAAF-1***. H_3btc (0.30 g, 1.4 mmol) was dissolved in DMF (10 mL) in a 20 mL glass vial. Then, teoa (1.16 g, 7.8 mmol) and solid $ZnCl_2$ (0.3 g, 2.2 mmol) were added to the reaction mixture, and the resulting solution was heated without stirring at 100 °C for 24 h. During this period, polyhedral crystals of **MOAAF-1** were formed. They were isolated by filtration, washed several times with DMF and diethylether, and dried under vacuum. Yield (based on H_3btc): ∼0.554 g (80%). The dried crystalline product was analyzed as **MOAAF-1**·H_2O. Anal. Calc. for $C_{24}H_{38}N_2O_{15}Zn$: C, 43.68; H, 5.83; N, 4.24. Found: C, 43.72; H, 5.75; N, 4.35%. Selected IR data (KBr pellet, cm^{-1}): 3376 (s), 2955 (w), 2891 (w), 1626 (s), 1583 (s), 1439 (s), 1359 (s), 1100 (s).

MOAAF-2−MOAAF-6. Compounds **MOAAF-2−MOAAF-6** were synthesized with a procedure similar to that for **MOAAF-1** with the exception that different amino-alcohols were used: hmpip for **MOAAF-2**, tbdeoa for **MOAAF-3**, bhep for **MOAAF-4**, mdeoa for **MOAAF-5**, and hem for **MOAAF-6**. The yields (based on H_3btc) were 0.382 g (70%), 0.438 g (75%), 0.332 g (65%), 0.449 g (80%),

Table 1. Selected Crystal Data for Compounds MOAAF-1−6

compound	MOAAF-1	MOAAF-2	MOAAF-3	MOAAF-4	MOAAF-5	MOAAF-6
empirical formula	$C_{24}H_{36}N_2O_{14}Zn$	$C_{37}H_{36}N_3O_{19}Zn_3$	$C_{41}H_{47}N_3O_{18}Zn_3$	$C_{49}H_{57}N_7O_{24}Zn_3$	$C_{39}H_{39}N_3O_{22}Zn_4$	$C_{41}H_{41}N_3O_{22}Zn_4$
formula weight	641.92	1022.80	1065.93	1324.19	1163.21	1189.25
crystal system	cubic	monoclinic	orthorhombic	trigonal	monoclinic	monoclinic
a/Å	20.413(5)	16.965(4)	14.2247(5)	43.8139(8)	23.314(2)	18.5152(4)
b/Å	20.413(5)	15.517(2)	32.481(3)	43.8139(8)	14.419(2)	15.2446(3)
c/Å	20.413(5)	14.073(2)	15.5954(9)	17.2006(3)	18.072(2)	21.4278(5)
α/°	90.00	90.00	90.00	90.00	90.00	90.00
β/°	90.00	108.12(2)	90.00	90.00	105.571(10)	100.999(2)
γ/°	90.00	90.00	90.00	120.00	90.00	90.00
V/Å^3	8506(4)	3520.8(9)	7205.7(8)	28595.5(9)	5852.0(11)	5937.0(2)
temperature/K	100(2)	100(2)	100(2)	100(2)	100(2)	100(2)
space group	$I\bar{4}3d$	*P2/c*	*Cmma*	$R\bar{3}$	*I2/a*	*I2/a*
Z	12	2	4	18	4	4
μ/mm^{-1}	0.939	1.062	1.039	1.202	1.687	1.665
total/independent reflections	25869/1251	16392/6208	22335/3355	11162/11162	17701/5151	19470/5227
R_{int}	0.0394	0.0604	0.0476	0.0000	0.1268	0.0608
$R_1{}^a/wR(F^2)^b$ ($I > 2\sigma(I)$)	0.0503/0.1457	0.0730/0.1967	0.0884/0.2662	0.0530/0.1422	0.0703/0.2084	0.0648/0.1923
GOF	1.097	0.891	1.050	1.034	1.108	1.075

$^aR_1 = \sum||F_o| - |F_c||/\sum|F_o|$. $^bwR(F^2)=[\sum[w(F_o^2 - F_c^2)^2]/\sum[wF_o^2)^2]]^{1/2}$, $w = 1/[\sigma^2(F_o^2) + (m\cdot p)^2 + n\cdot p]$, $p = [\max(F_o^2,0) + 2F_c^2]/3$, and *m* and *n* are constants.

dx.doi.org/10.1021/cg301047w | *Cryst. Growth Des.* 2012, 12, 5471−5480

and 0.417 g (75%) for **MOAAF-2**, **MOAAF-3**, **MOAAF-4**, **MOAAF-5**, and **MOAAF-6**, respectively. The dried crystalline product for compound **MOAAF-2** was analyzed as **MOAAF-2**·DMF·$4H_2O$. Anal. Calc. for $C_{40}H_{54}N_4O_{24}Zn_3$: C, 41.02; H, 4.65; N, 4.78. Found: C, 41.12; H, 4.55; N, 4.68%. Selected IR data (KBr pellet, cm^{-1}): 3412 (s), 2964 (w), 2794 (w), 1672 (s), 1595 (s), 1355 (s). The dried crystalline product for compound **MOAAF-3** was analyzed as **MOAAF-3**·2DMF·$2H_2O$. Anal. Calc. for $C_{47}H_{67}N_5O_{22}Zn_3$: C, 45.15; H, 5.40; N, 5.60. Found: C, 45.02; H, 5.45; N, 5.68%. Selected IR data (KBr pellet, cm^{-1}): 3452 (s), 2814 (w), 1606 (s), 1585 (s), 1357 (s). The dried crystalline product for compound **MOAAF-4** was analyzed as **MOAAF-4**·$3H_2O$. Anal. Calc. for $C_{37}H_{43}N_3O_{23}Zn_3$: C, 40.62; H, 3.96; N, 3.84. Found: C, 40.42; H, 3.82; N, 3.95%. Selected IR data (KBr pellet, cm^{-1}): 3444 (s), 2953 (w), 1664 (s), 1635 (s), 1358 (s). The dried crystalline product for compound **MOAAF-5** was analyzed as **MOAAF-5**·$2H_2O$. Anal. Calc. for $C_{39}H_{47}N_3O_{24}Zn_4$: C, 38.92; H, 3.94; N, 3.49. Found: C, 39.05; H, 3.87; N, 3.55%. Selected IR data (KBr pellet, cm^{-1}): 3448 (s), 2923 (w), 1624 (s), 1573 (s), 1442 (s), 1362 (s). The dried crystalline product for compound **MOAAF-6** was analyzed as **MOAAF-6** (no solvent molecules were found). Anal. Calc. for $C_{41}H_{43}N_3O_{22}Zn_4$: C, 41.33; H, 3.64; N, 3.53. Found: C, 41.25; H, 3.68; N, 3.45%. Selected IR data (KBr pellet, cm^{-1}): 3450 (s), 2923 (w), 1624 (s), 1575 (s), 1444 (s), 1364 (s). The purity of all products was also confirmed by the comparison of the experimental powder X-ray diffraction patterns to those calculated from the single crystal X-ray data (see Figures S1–S6 in the Supporting Information).

Single Crystal X-ray Crystallography. Single crystal X-ray diffraction data were collected on an Oxford-Diffraction Supernova diffractometer, equipped with a CCD area detector utilizing Mo Kα (λ = 0.71073 Å) radiation. Suitable crystals were attached to glass fibers using paratone-N oil and transferred to a goniostat where they were cooled for data collection. Empirical absorption corrections (multiscan based on symmetry-related measurements) were applied using CrysAlis RED software.[32] The structures were solved by direct methods using SIR2004[33] and refined on F^2 using full-matrix least-squares using SHELXL97.[34] Software packages used: CrysAlis CCD for data collection,[32] CrysAlis RED for cell refinement and data reduction,[32] WINGX for geometric calculations,[35] and DIAMOND[36] for molecular graphics. The non-H atoms were treated anisotropically, whereas the H atoms were placed in calculated, ideal positions and refined as riding on their respective carbon atoms. Electron density contributions from disordered guest molecules were handled using the SQUEEZE procedure from the PLATON software suit.[37a] The solvent accessible volumes and the sizes of the cavities were calculated using the CALC SOLV and CAVITY PLOT utilities of PLATON, respectively.[37a] Topological analysis was performed with the aid of TOPOS.[37b] The structure of **MOAAF-4** was refined as a non-merohedral twin using the HKLF 5 option in SHELXL-97.[34] CCDC 893091–893096 contain the supplementary crystallographic data for this paper. These data can be obtained free of charge via www.ccdc.cam.ac.uk/data_request/cif. Selected crystal data for all compounds are given in Table 1.

RESULTS AND DISCUSSION

Synthesis. As mentioned in the introduction, our group has been investigating the use of polytopic organic ligands together with various amino-alcohols as a method for the synthesis of new MOFs. In this work, we report the initial results of these investigations that involve the employment of the well-known tricarboxylic ligand H_3btc that has afforded so far a number of interesting porous MOFs[1,3] in combination with amino-alcohols that can be potential templates to direct the assembly of new MOFs[23] or ligands to build novel SBUs.[29] Thus, reaction of $ZnCl_2$, H_3btc, and teoa in a molar ratio 1.6:1:5.6 in DMF at 100 °C resulted in compound **MOAAF-1** in ~80% yield (Scheme 2). Similar reactions with the amino-alcohols hmpip, tbdeoa, bhep, mdeoa, and hem led to compounds **MOAAF-2**–**MOAAF-6**, respectively, as summarized in Scheme 2 in 50–80% yields.

Scheme 2. Synthetic Routes Leading to Compounds MOAAF-1–6

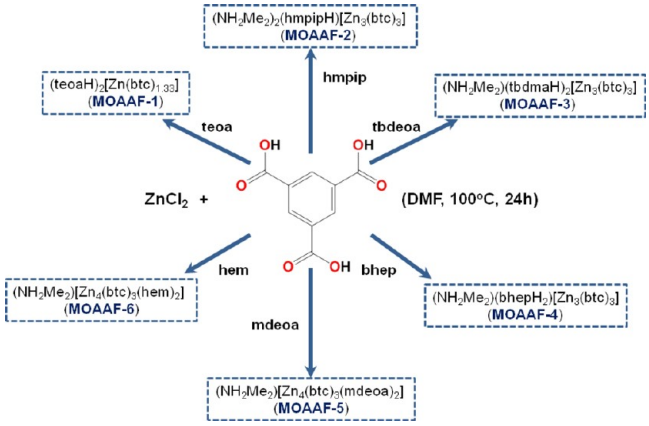

As shown in this scheme, teoa, hmpip, and bhep acted as bases and their protonated forms templated the assembly of compounds **MOAAF-1**, **2**, and **4**, respectively (see also the description of the crystal structures). Similarly, in the case of **MOAAF-3** the cation of *tert*-butyl-dimethylammonium ($tbdmaH^+$) that was formed in situ, possibly from the decomposition of tbdeoa, also serves as both a template and a countercation. On the other side, mdeoa and hem acted as chelating ligands for the Zn^{2+} ions (see also description of the crystal structures). In addition, all compounds (with the exception of **MOAAF-1**) contain dimethylammonium counter cations resulted from the decomposition of DMF. The purity of the products was confirmed by the similarity between the experimental and calculated (from single crystal diffraction data) PXRD patterns (Figures S1–S6 in the Supporting Information). Several reactions were performed with a variety of $ZnCl_2$:H_3btc:amino-alcohol ratios which revealed that in all cases a large excess of amino-alcohol ligands was essential in order to obtain the desired compound in high purity and decent yield. Compounds **MOAAF-1**–**MOAAF-6** were also isolated when other Zn^{2+} salts (e.g., $Zn(NO_3)_2$, $Zn(O_2CMe)_2$, etc) were used in place of $ZnCl_2$. Reactions were also performed without the presence of amino-alcohols and the product obtained in all cases was the known compound $(Me_2NH_2)[Zn(btc)]$·DMF.[38]

Crystal Structure of MOAAF-1. Representations of the secondary building unit (SBU)/3D structure and net topology of **MOAAF-1** are shown in Figures 1 and 2, respectively. Compound **MOAAF-1** is a 3D coordination polymer that crystallizes in the cubic space group $I\bar{4}3d$. Its repeating unit consists of one crystallographically unique Zn^{2+} ion coordinated in distorted tetrahedral geometry by four carboxylic oxygen atoms from four different btc^{3-} ligands (Figure 1a), with each btc^{3-} ligand connected to three Zn^{2+} ions. The tetrahedral $[Zn(COO)_4]^{2-}$ units are interconnected through btc^{3-} ligands, creating a three-dimensional framework with the ligands and Zn^{2+} ions representing 3- and 4-connected nodes, respectively (Figures 1b and 2).

The point symbol for this net is $(8^3)_4(8^6)_3$ corresponding to the known **ctn** network topology (Figure 2). The negative charge of the $[Zn(btc)_{1.33}]^{2-}$ framework is balanced by $teoaH^+$ cations filling the pores of **MOAAF-1**. It should be noted that

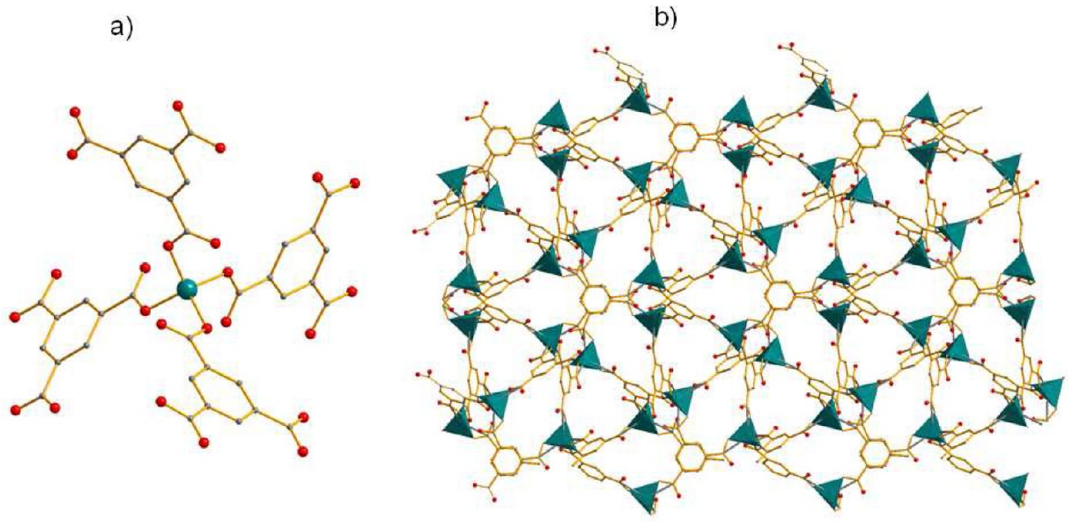

Figure 1. (a) Coordination environment of Zn^{2+} ions (Zn, green; C, gray; O, red) and (b) the 3D structure of **MOAAF-1** viewed along [111] with the green polyhedra representing the ZnO_4 tetrahedra (guests are not shown).

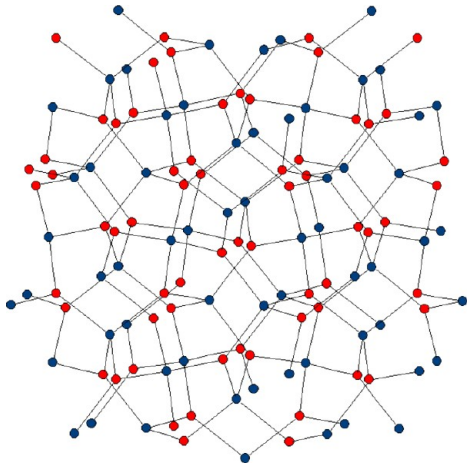

Figure 2. Representation of the **ctn**-net (blue and red balls correspond to the 4- and 3-c nodes, respectively) of **MOAAF-1**.

teoaH$^+$ cations were severely disordered and could not be modeled properly with the refinement of the crystal structure. However, their presence was undoubtedly confirmed by ^{1}H NMR spectroscopic data for a sample of **MOAAF-1** digested in concentrated acid (Figure S7 in the Supporting Information). The solvent-accessible volume of **MOAAF-1** calculated by PLATON[37a] (excluding all cations and solvents from the pores) is 5547.2 Å^3, corresponding to 65.2% of the unit cell volume. The 3D structure contains cavities with diameters ∼6 Å as found by PLATON (taking into account the van der Waals radii of the atoms).[37a] A representation of the pore network of **MOAAF-1** with the structure visualization program MERCURY[39] reveals a continuous and complex 3D pore network, where the cavities communicate through wide channels with a diameter ≥4 Å (Figure S8 in the Supporting Information).

There are several MOFs with a **ctn** network topology, the majority of which are M^{3+}-btc^{3-} MOFs.[23,40,41] Interestingly, one of these MOFs, compound $(teoaH)_3[In_3(btc)_4]$ contains teoaH$^+$ counter cations as **MOAAF-1**.[23] Other examples of polymeric species that display a **ctn** structural topology include a Ga^{3+}-btc^{3-} compound,[41] a Cd^{2+}[42] and a Mn^{2+}-aminotetrazole[43] MOFs, a Ag^+-*cis,cis*-1,3,5-triaminocyclohexane compound,[44] a series of lanthanide MOFs,[45] a doubly interpenetrated Cu^{2+} polymer[46a], and Be^{2+}-containing MOF.[46b]

Crystal Structures of MOAAF-2 and 3. Compounds **MOAAF-2** and **3** display related structures (with their main difference being the type of counter cations) and thus only the structure of **MOAAF-2** will be discussed in detail. Representations of the SBUs/3D structure and net topology of **MOAAF-2** are shown in Figures 3 and 4, respectively. **MOAAF-2** crystallizes in the monoclinic space group *P*2/*c*. It contains two crystallographically unique Zn^{2+} ions coordinated by four carboxylic oxygen atoms and adopting a distorted tetrahedral geometry as well as two types of btc^{3-} ligands (with stoichiometry 2:1) both exhibiting a μ_4 coordination mode. Two kinds of repeating units are recognized in the structure of **MOAAF-2**, a mononuclear $[Zn(COO)_4]^{2-}$ unit containing a distorted tetrahedral Zn^{2+} center and a dinuclear $[Zn_2(COO)_5]^{-1}$ (Figure 3a) SBU. The latter consists of two crystallographically equivalent Zn^{2+} ions coordinated by three μ_2- and two monodentate COO^- groups and appears for the first time in MOFs chemistry. In particular, a search in the Cambridge Structural Database revealed that the $[M_2(COO)_5]$ (M = any metal ion) unit present in **MOAAF-2** is quite uncommon presented only in the (H_2NMe_2)-$[Zn_2(O_2CNMe_2)_5]$·MeCN compound that is a discrete dinuclear complex[47] and in a Co_{17} metal cluster.[48]

The interconnection of the repeating units via the btc^{3-} ligands leads to a (3,3,4,5)-connected net, in which there are two types of 3-c nodes (the two types of btc^{3-} ligands) as well as 4-c and 5-c nodes corresponding to $[Zn(COO)_4]^{2-}$ and dinuclear $[Zn_2(COO)_5]^{-1}$ SBUs, respectively. The point symbol for this net is $(4.8^2)_2(4^2.6.8^5.10^2)(4^2.6)(4^2.8^4)$ and represents a unique topology (Figure 4).

The 3D structure contains two types of cavities; the first one displays a hexagonal shape and relatively large diameters ∼9−10 Å and the second one rhombic shape and smaller diameters ∼4−5 Å as found by PLATON[37a] (taking into account the van der Waals radii of the atoms), Figure 3c. The pores accommodate protonated hmpipH$^+$ ions (positionally disordered over two positions) that are involved in hydrogen bonding interactions (2.6−2.7 Å) via their N and OH groups

dx.doi.org/10.1021/cg301047w | *Cryst. Growth Des.* 2012, 12, 5471−5480

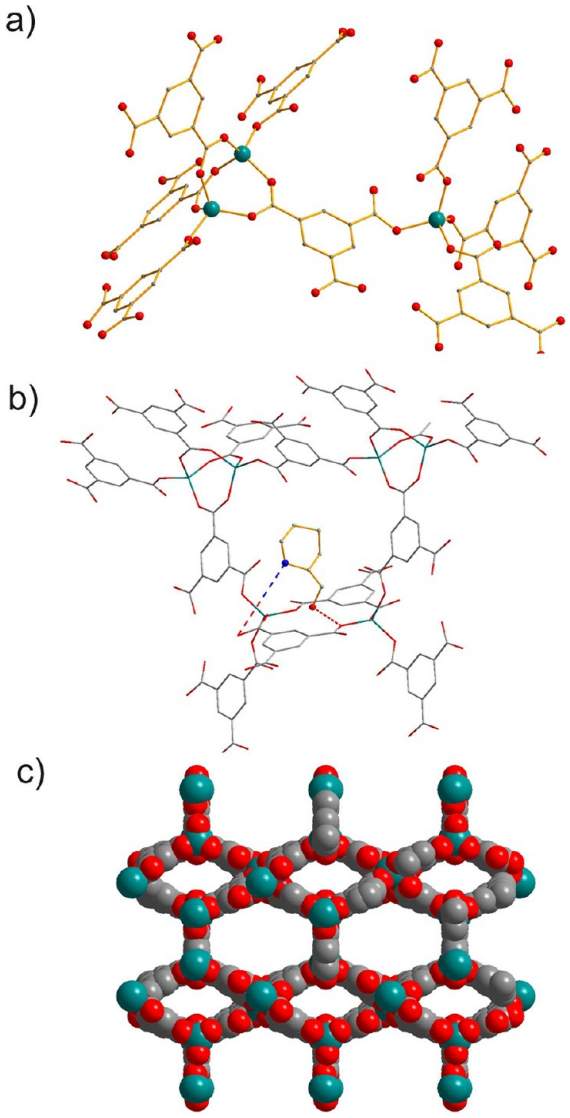

Figure 3. Representation of (a) the SBUs, (b) a cavity hosting the $hmpipH^+$ cation (hydrogen bonds are shown with dashed lines), and (c) the space-filling model of the 3D structure of **MOAAF-2** viewed down the *c*-axis (guests are not shown for clarity). Color code: Zn, green; C, gray; O, red; N, blue.

with carboxylic oxygen atoms of the btc^{3-} ligands (Figure 3b) as well as $[NH_2Me_2]^+$ cations and lattice solvents.

The solvent-accessible volume of **MOAAF-2** calculated by PLATON[37a] (after refining the structure excluding all cations and solvents from the pores) is 2387 Å^3, corresponding to 67.8% of the unit cell volume. The pore network of **MOAAF-2** is continuous, and the cavities are connected through wide channels with a diameter of ≥4 Å as found with MERCURY (Figure S9 in the Supporting Information).[39]

As mentioned above, compounds **MOAAF-2** and **-3** exhibit similar structures. Their main differences lie in the crystal systems and space groups in which these compounds crystallize (monoclinic *P*2/*c* for **MOAAF-2** and orthorhombic *Cmma* for **MOAAF-3**) and the type of counter cations ($hmpipH^+$/$[NH_2Me_2]^+$ for **MOAAF-2** and $tbdmaH^+$/$[NH_2Me_2]^+$ for **MOAAF-3**) located in their pores. Interestingly, $tbdmaH^+$ which was not used in the reaction mixture that resulted in **MOAAF-3** and formed *in situ* possibly from the decomposition of tbdeoa, appears for the first time in a crystal structure (Figure S10 in the Supporting Information), as revealed by a search in the Cambridge Structural Database.

Crystal Structure of MOAAF-4. Representations of the SBUs/3D structure and net topology of **MOAAF-4** are shown in Figures 5 and 6, respectively. Compound **MOAAF-4** crystallizes in the trigonal space group $R\bar{3}$. Its asymmetric unit contains three crystallographically unique Zn^{2+} centers, three independent btc^{3-} ligands, one $bhepH_2^{2+}$, one $[NH_2Me_2]^+$, and four DMF lattice molecules. There are two types of repeating units in the structure, a mononuclear $[Zn(COO)_4]^{2-}$ one containing a tetrahedral Zn^{2+} ion linked to four $O_{carboxylate}$ atoms coming from four different btc^{3-} ligands and a dinuclear $[Zn_2(COO)_5]^{-1}$ SBU (Figure 5a). The $[Zn_2(COO)_5]^{-1}$ SBU is asymmetric since one of its Zn^{2+} ions is ligated to three μ_2- and one *monodentate* COO^- groups adopting a distorted tetrahedral geometry, whereas the second one is coordinated to three μ_2- and one *chelating* COO^- groups adopting a distorted trigonal bipyramidal geometry. The main difference between the dinuclear SBUs of **MOAAF-4** and those in **MOAAF-2** and **-3** compounds lies in the fact that the SBUs in the latter MOFs are symmetric containing two Zn^{2+} ions that adopt a distorted tetrahedral geometry (see above).

The interconnection of the repeating units via the btc^{3-} ligands results in a (3,3,4,5)-connected net, in which there are two types of 3-c nodes (the btc^{3-} ligands) as well as 4-c and 5-c nodes corresponding to $[Zn(COO)_4]^{2-}$ and dinuclear $[Zn_2(COO)_5]^{-1}$ SBUs, respectively (Figure 6). The point symbol for this net is $(6^3)_3(6^4.8^2)(6^6.8^2.10^2)$ and represented a unique network topology until very recently, when another Zn^{2+}-btc^{3-} MOF, compound $[NH_2Me_2]^+[Zn_3(btc)_3]\cdot 4DMA$ (DMA = dimethylacetamide) found to adopt the exact same topology (and also similar SBUs as those in **MOAAF-4**).[49]

The 3D structure contains large wheel-shaped and hexagonal cavities with diameters ∼7−10 Å as found by PLATON[37a] (taking into account the van der Waals radii of the atoms), Figure 5c. The hexagonal pores accommodate deprotonated $bhepH_2^{2+}$ ions (Figure 5b) that are involved in hydrogen bonding interactions (2.7 Å) via their OH groups with carboxylic oxygen atoms of the btc^{3-} ligands and via their N atoms with O atoms of DMF guest molecules also hosted in these pores. The wheel-shaped cavities contain $[NH_2Me_2]^+$ cations and DMF guest molecules which are also involved in hydrogen bonding interactions (the N atom of $[NH_2Me_2]^+$ cation is hydrogen bonded to the O atoms of a DMF and a btc^{3-} molecules).

The solvent-accessible volume of **MOAAF-4** calculated by PLATON[37a] (excluding all cations and solvents from the pores) is 18211.5 Å^3 corresponding to 63.7% of the unit cell volume. The representation of the voids of **MOAAF-4** with MERCURY[39] revealed a continuous pore network, in which the cavities are connected through wide channels with a diameter ≥4 Å (Figure S11 in the Supporting Information).

Crystal Structures of MOAAF-5 and -6. Compounds **MOAAF-5** and **-6** display related structures (with the exception of the type of the amino-alcohol ligand) and thus, only the structure of **MOAAF-5** will be discussed in detail. Representations of the SBUs/3D structure and net topology of **MOAAF-5** are shown in Figures 7 and 8, respectively. **MOAAF-5** crystallizes in the monoclinic space group *I*2/*a* with its asymmetric unit consisting of two crystallographically unique Zn^{2+} centers, two types of btc^{3-} ligands (with stoichiometry 2:1), one mdeoa ligand, as well as disordered $[NH_2Me_2]^+$ cations and solvent molecules. The structure is based on two

dx.doi.org/10.1021/cg301047w | *Cryst. Growth Des.* 2012, 12, 5471−5480

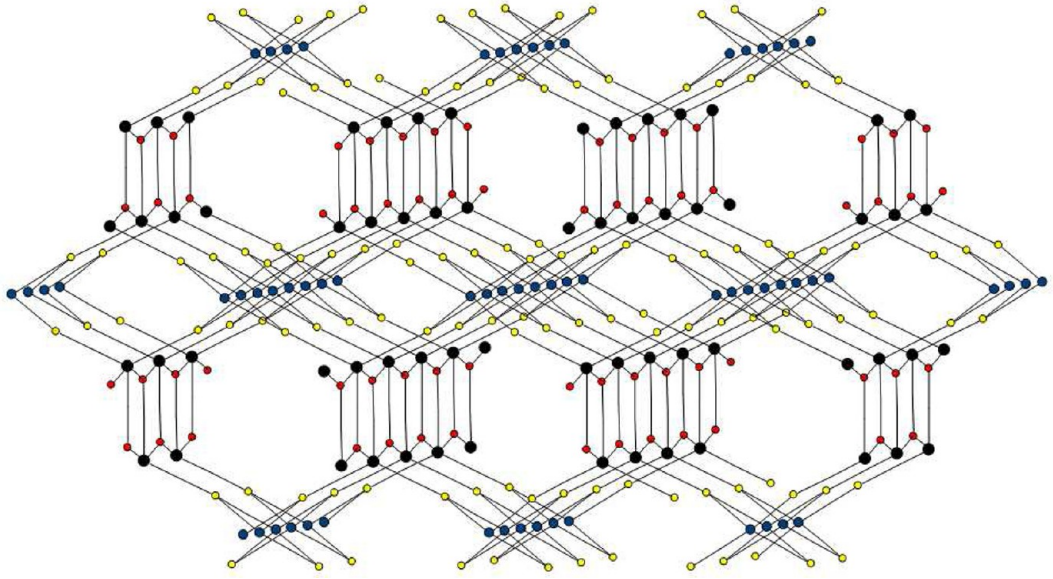

Figure 4. Representation of the unique (3,3,4,5)-connected net of **MOAAF-2** and -**3**. Color code: 3-c nodes (one type), yellow; 3-c nodes (second type), red; 4-c nodes, blue; 5-c nodes, black.

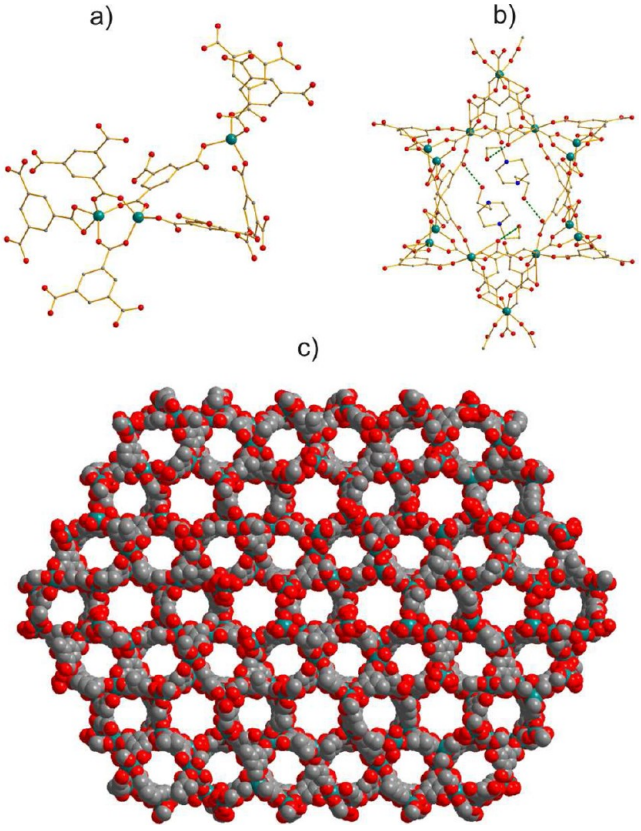

Figure 5. Representation of (a) the SBUs, (b) a hexagonal cavity hosting two $bhepH_2^{2+}$ cations (hydrogen bonds are drawn as dashed lines; DMF solvents in this cavity are not shown), and (c) the space filling model for the 3D structure of **MOAAF-4** viewed down the *c*-axis (guests were removed for clarity). Color code: Zn, green; C, gray; O, red; N, blue.

types of repeating units, a mononuclear $[Zn(COO)_2(mdeoa)]$ and a dinuclear $[Zn_2(COO)_5]^{-1}$ units. The Zn^{2+} ion of the mononuclear unit is coordinated by one chelating and one monodentate COO^- groups and a tridentate mdeoa ligand (i.e., connected via its amine and two hydroxyl groups), adopting an octahedral coordination geometry (Figure 7a) whereas the dinuclear SBU is very similar to those appeared in **MOAAF-2** and -**3**, described in a previous paragraph.

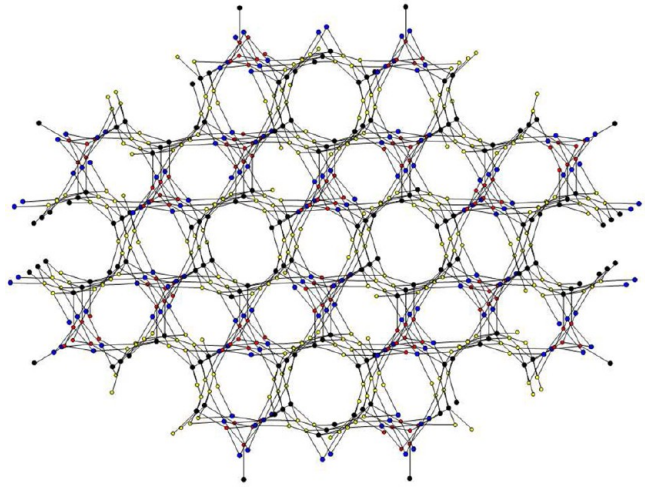

Figure 6. Representation of the (3,3,4,5)-connected net of **MOAAF-4**. Color code: 3-c nodes (one type), yellow; 3-c nodes (second type), red; 4-c nodes, blue; 5-c nodes, black.

The interconnection of the repeating units via the btc^{3-} ligands leads to a trinodal (3,3,5)-connected net, in which there are two types of 3-c nodes (the btc^{3-} ligands) and 5-c nodes corresponding to the $[Zn_2(COO)_5]^{-1}$ SBUs, Figure 8. The $[Zn(COO)_2(mdeoa)]$ units simply bridge between the two types of btc^{3-} ligands and therefore, are topologically silent. The point symbol for this net is $(4.6.8)_2(4^2.6^2.8^4.10^2)(6^2.8)$ and represents a unique topology. The 3D structure contains cavities with diameters ~4−5 Å as found by PLATON[37a] (taking into account the van der Waals radii of the atoms), Figure 7b. The solvent-accessible volume of **MOAAF-5** calculated by PLATON[37a] (excluding all cations and solvents from the pores) is 2211 $Å^3$, corresponding to 37.8% of the unit cell volume.

dx.doi.org/10.1021/cg301047w | *Cryst. Growth Des.* 2012, 12, 5471−5480

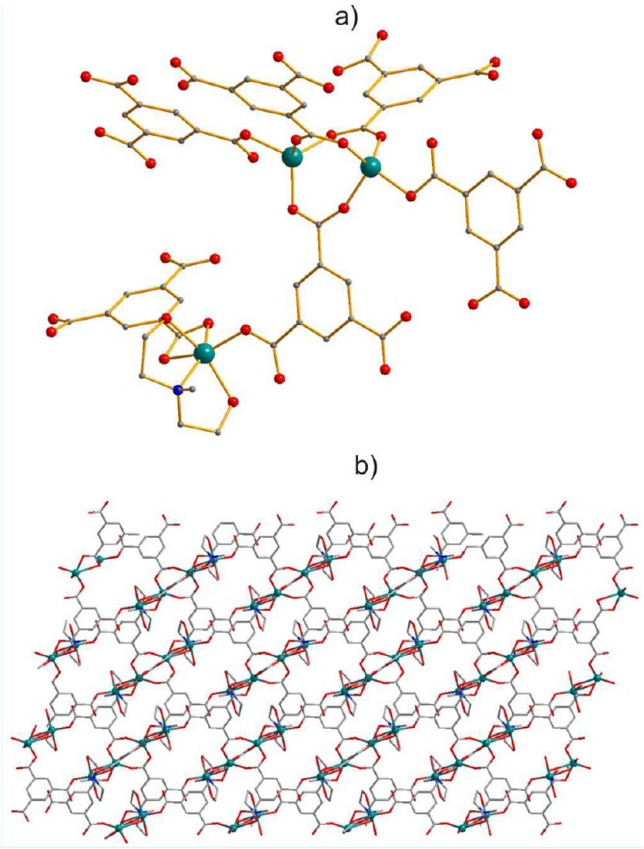

Figure 7. Representation of the (a) SBUs and (b) 3D structure of **MOAAF-5** viewed down the *b*-axis (guests are not shown). Color code: Zn, green; C, gray; O, red; N, blue.

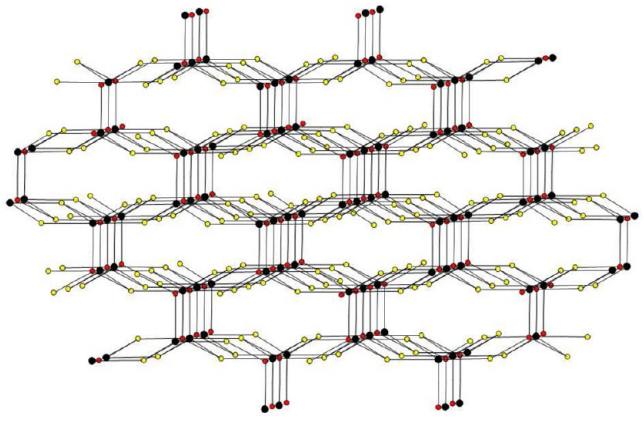

Figure 8. Representation of the unique (3,3,5)-connected net of **MOAAF-5** and **-6**. Color code: 3-c nodes (one type), yellow; 3-c nodes (second type), red; 5-c nodes, black.

The representation of the voids of **MOAAF-5** with MERCURY[39] revealed that the pores are connected through narrow passages that are ~3.2 Å wide (Figure S12 in the Supporting Information). The structure of **MOAAF-6** is very similar to that of **MOAAF-5**, as mentioned above. The main differences between them are (a) the type of the amino-alcohol ligand being mdeoa for **MOAAF-5** and hem for **MOAAF-6** and (b) the coordination geometry adopted by the Zn^{2+} ions connected with the amino-alcohol, which is octahedral $[Zn(COO)_2(mdeoa)]$ in the structure of **MOAAF-5** and square-pyramidal $[Zn(COO)_2(hem)]$ (with three carboxylate and one OH groups in the equatorial plane and one axial amine ligand) in the structure of **MOAAF-6** (Figure S13 in the Supporting Information). Finally, in both compounds the amino-alcohols (mdeoa and hem) are neutral, a fact that is supported by the charge balance requirements, the inspection of bond distances and bond valence sum (BVS) calculations[6] for the coordinated O atoms of the amino-alcohols indicating BVS values of 1.2−1.3 typical of OH groups.

Comparison of MOAAF-1 - MOAAF-6 with Reported Zn-btc MOFs. At this point, it is worthy comparing the structures of **MOAAF-1**−**MOAAF-6** with those of other Zn-btc MOFs reported in the literature. A Cambridge database search revealed that there are 31 Zn-btc MOFs containing the tricarboxylic ligand as the only type of bridging ligand.[14,38,49−75]

Selected structural data for all Zn-btc MOFs are provided in Table 2. This comparison revealed that all coordination modes for btc^{3-} found in **MOAAF-1**−**MOAAF-6**, shown in Scheme 3 (**MOAAF-1**, B; **MOAAF-2** and **3**, A; **MOAAF-4**, A and D; **MOAAF-5**, A and C; **MOAAF-6**, A and D;) have been already appeared in Zn-btc MOFs. In particular, the coordination modes A, B, and D shown in Scheme 3 have been frequently observed,[60] whereas mode C has been appeared in only one other example.[76]

Comparing the topological features of compounds **MOAAF-1**−**MOAAF-6** with those of known Zn-btc MOFs (Table 2), it was realized that **MOAAF-1** is the only Zn-btc MOF with a **ctn** network topology and, more importantly, compounds **MOAAF-2**−**MOAAF-6** display 3- or 4-nodal nets and rare or unprecedented structural topologies, whereas the reported Zn-btc compounds with 3D structures show binodal (3,4, 3,5, or 3,6)-nets with only one exception being compound $[NH_2Me_2]^+[Zn_3(btc)_3]\cdot 4DMA$ which displays similar topology to that of **MOAAF-4** (see above).[49] It is remarkable that **MOAAF-1**−**MOAAF-6** exhibit new topological characteristics compared to known Zn-btc MOFs, taking into account that the observed btc^{3-} connectivity modes in **MOAAF-1**−**MOAAF-6** have been reported for several Zn-btc compounds. The novel topological features of **MOAAF-1**−**MOAAF-6** have probably resulted from the presence of unprecedented or rare SBUs (dinuclear units in compounds **MOAAF-2**−**MOAAF-4**) in combination with the templating effect (compounds **MOAAF-1**−**MOAAF-4**) and ligation (compounds **MOAAF-5** and **-6**) of the amino-alcohols.

Thermal Stability Studies. The thermal stability of **MOAAF-1**−**MOAAF-6** was investigated by means of the thermogravimetric analysis (TGA) technique. The TG/DTG (1st derivative) data for compounds **MOAAF-1**−**MOAAF-5** show weight losses from 20 °C to temperatures 100−200 °C assigned to the removal of lattice solvents (H_2O or/and DMF), whereas **MOAAF-6** displays no losses at this temperature range (Figures S14−S19 in the Supporting Information). At higher temperatures, all compounds exhibit a series of weight losses attributed to the elimination of organic cations, amino-alcohols, and btc^{3-} ligands. The decomposition of the compounds is completed at temperatures in between 600 and 830 °C. A detailed description of the thermal analyses data for **MOAAF-1** - **MOAAF-6** and the TG/DTG diagrams (Figures S14−S19) are provided in the Supporting Information.

Photoluminescence (PL) Studies. The PL properties of compounds **MOAAF-1**−**MOAAF-6** were investigated at room temperature. The H_3btc ligand exhibits a strong emission at ~380 nm when excited at 343 nm that is attributed to a $\pi^* \rightarrow n$ transition, whereas the amino-alcohols (teoa, hmpip, tbdeoa,

dx.doi.org/10.1021/cg301047w | *Cryst. Growth Des.* 2012, 12, 5471−5480

Table 2. Selected Structural Data for Zn-btc Compounds from the Literature and the Present Work

compound	dimensionality	coordination mode	net	ref
Zn(Hbtc)	1D	μ_2	N/A	50
Zn(btc)	2D	μ_3	4.8^2	14, 51
Zn(btc)	1D	μ_2	N/A	52
Zn(btc)	3D	μ_4	3,6 (rutile) $(4.6^2)_2(4^2.6^{10}.8^3)$	38
$Zn_3OH(btc)_2$	3D	μ_5	3,6	53
$Zn_3OH(btc)_2$	3D	μ_5,μ_4	3,6 $(4.6^2)(6^3)(4.6^{11}.8^3)$	54
$Zn_3OH(btc)_2$	3D	μ_4	N/A	55
$Zn_3OH(btc)_2$	3D	μ_5	N/A	56
$Zn_3(btc)_2$	3D	μ_5, μ_6	3,4-$(6^3)_4(6^2.8^2.10^2)(6^4.8^2)_2$	57
$Zn_3(btc)_2$	3D	μ_5, μ_6	3,4-$(4\cdot6\cdot8)_2(6\cdot6\cdot8^2)_2(6\cdot6\cdot8\cdot8\cdot10^4\cdot*)(4\cdot6\cdot6\cdot8\cdot8\cdot10^4)_2$	58
$Zn_3(btc)_2$	3D	μ_5	N/A	59
$Zn_3(btc)_2$	3D	μ_6	N/A	60
$Zn_3(btc)_2$	3D	μ_3	N/A	61
$Zn_3(btc)_2$	2D	μ_3	4.8^2	62, 63
$Zn_3(btc)_2$	1D	μ_3	N/A	64
$Zn_3(btc)_2$	1D	μ_2, μ_3	N/A	65
$Zn_2OH(btc)$	3D	μ_6	N/A	66
$Zn_2(OH)I(btc)$	3D	μ_5	N/A	67
$Zn_2(Hbtc)(btc)$	3D	μ_3, μ_4	3,5-$(6^3)(6^9.8)$	68
$Zn_2(OH)Br(btc)$	3D	μ_5	N/A	60
$Zn_2(NO_3)(btc)$	3D	μ_6	N/A	69
$Zn_2(btc)$-Zn(btc)	1D	μ_2, μ_3	N/A	70a
$Zn_2(btc)_{1.33}$	3D	μ_6	N/A	70b
$Zn_2(btc)$-$Zn_2(btc)_{1.33}$	3D	μ_6	N/A	70b
$Zn_4(OH)_2(btc)_2$	3D	μ_6	N/A	71
$Zn_4(OH)(btc)_3$	3D	μ_3, μ_6	N/A	60
$Zn_4(Hbtc)_2$	2D	μ_2, μ_4	N/A	63
$Zn_4(O)(btc)_2$	3D	μ_6	3,6	72
$Zn_6(btc)_4$	3D	μ_5, μ_6	3,4-$(6\cdot6\cdot6)_4(6^2\cdot6^2\cdot8^2\cdot8^2\cdot12^2\cdot12^2)_2(6^2\cdot6^2\cdot8\cdot8\cdot8\cdot8)$	58
$Zn_6O_2(btc)_4$	3D	μ_5	3,4	73
$Zn_6(OH)_3(btc)_3$	3D	μ_6	N/A	74
$Zn_7(OH)_2(btc)_4$	3D	μ_4, μ_6	N/A	75
$Zn_{12}(OH)_4(btc)_8$	3D	μ_5, μ_6	3,6-$(4.6^2)_2(4^2.6^{10}.8^3)$	68
$Zn_3(btc)_3$	3D	μ_4	3,3,4,5-$(4.8^2)_2(4^2.6.8^5.10^2)(4^2.6)(4^2.8^4)$	this work
$Zn(btc)_{1.33}$	3D	μ_3	$(8^3)_4(8^6)$ (ctn)	this work
$Zn_3(btc)_3$	3D	μ_4	3,3,4,5-$(6^3)_3(6^4.8^2)(6^6.8^2.10^2)$	this work and ref 49
$Zn_4(btc)_3$	3D	μ_4	3,3,5-$(4.6.8)_2(4^2.6^2.8^4.10^2)(6^2.8)$	this work

Scheme 3. Coordination Modes of btc^{3-} in Compounds MOAAF-1—MOAAF-6

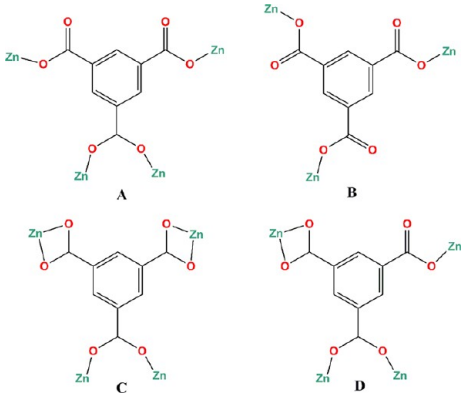

mdeoa, hem, and bhep) showed no PL emissions. Compounds **MOAAF-2** and **-5** display emission peaks at 405 (exc. 340 nm) and 430 nm (exc. 360 nm), respectively (Figure 9). Thus, the emission wavelengths of **MOAAF-2** and **-5** are significantly red-shifted compared to that of free H_3btc ligand, and this is

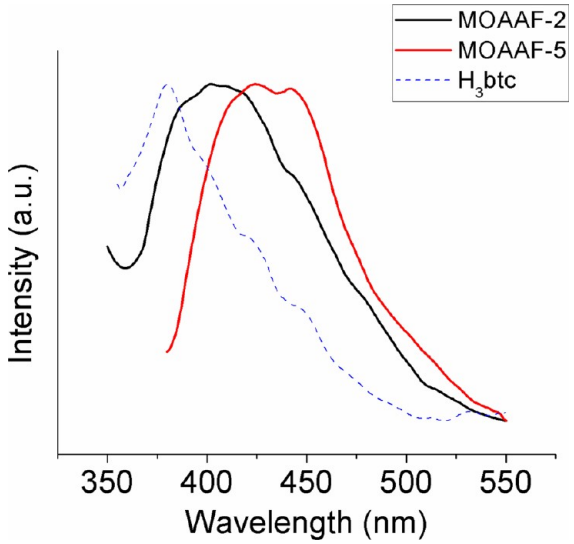

Figure 9. Emission spectra for H_3btc (exc. 343 nm), **MOAAF-2** (exc. 340 nm), and **MOAAF-5** (exc. 360 nm).

dx.doi.org/10.1021/cg301047w | *Cryst. Growth Des.* 2012, 12, 5471−5480

probably caused by a ligand-to-metal charge transfer (LMCT).[66] On the other side, **MOAAF-1**, **-3**, **-4**, and **-6** show very weak emissions when excited at ~340 nm. The inconsistency in the emissions of **MOAAF-1**–**MOAAF-6** is probably due to their differences in the coordination environment of Zn^{2+} ions and/or their different counter cations and lattice solvents.

CONCLUSIONS

In conclusion, a series of new Zn^{2+} MOFs (**MOAAF-1**–**MOAAF-6**) have been isolated from reactions that involved use of a combination of H_3btc with the amino-alcohols teoa, hmpip, tbdeoa, mdeoa, hem, and bhep. All compounds showed 3D structures with relatively large pores (4–10 Å) and solvent-accessible volumes (38–68% of the unit cell volumes) and displayed a number of unprecedented structural features, such as novel SBUs and unique network topologies. Taking into account that over 30 Zn-btc MOFs and numerous other 3d metal-btc compounds are known and almost all possible connectivity modes of btc^{3-} have been already reported, it is remarkable that four of the six MOFs presented in this work exhibit novel network topologies. Clearly, amino-alcohols played a key role in the isolation of MOFs with novel structural characteristics as were shown to act with various different ways, e.g. as bases (teoa, hmpip, bhep), templates (teoa, hmpip, bhep), or chelating ligands (mdeoa, hem). This study represents the initial systematic investigation on the use of a combination of a polytopic ligand and an aminoalcohol for the isolation of MOFs and demonstrates it as an efficient synthetic method for the isolation of novel MOFs, even when well-known polytopic ligands are employed. In addition, it provides insights on the sensitivity of the synthesis of MOFs not only to reaction conditions but also to the additives present in the reaction solution. Given the plethora of polytopic ligands and amino-alcohols, a large number of MOFs with new structural features and potentially interesting physical properties may be obtained by their proper combination. By applying this synthetic method, we have already prepared a large number of new MOFs that will be reported in future papers.

ASSOCIATED CONTENT

Supporting Information

PXRD, structural data and figures, and thermal analyses data. This material is available free of charge via the Internet at http://pubs.acs.org.

AUTHOR INFORMATION

Corresponding Author

*Tel.: ++357-22-892765. Fax: ++357-22-895451. E-mail: gspapaef@chem.uoa.gr (G.S.P.); atasio@ucy.ac.cy (A.J.T).

Notes

The authors declare no competing financial interest.

ACKNOWLEDGMENTS

This work was supported by the Cyprus Research Promotion Foundation Grants ΔΙΔΑΚΤΩΡ/ΔΙΣΕΚ/0308/22 and ΔΙ-ΔΑΚΤΩΡ/0609/43 which are cofunded by the Republic of Cyprus and the European Regional Development Fund.

REFERENCES

(1) Eddaoudi, M.; Moler, D. B.; Li, H. L.; Chen, B. L.; Reineke, T. M.; O'Keeffe, M.; Yaghi, O. M. *Acc. Chem. Res.* **2001**, *34*, 319.
(2) Ferey, G. *Chem. Soc. Rev.* **2008**, *37*, 191.
(3) Bradshaw, D.; Claridge, J. B.; Cussen, E. J.; Prior, T. J.; Rosseinsky, M. J. *Acc. Chem. Res.* **2005**, *38*, 273.
(4) Horike, S.; Shimomura, S.; Kitagawa, S. *Nat. Chem.* **2009**, *1*, 695.
(5) Ma, L. Q.; Falkowski, J. M.; Abney, C.; Lin, W. B. *Nat. Chem.* **2010**, *2*, 838.
(6) Moushi, E. E.; Stamatatos, T. C.; Wernsdorfer, W.; Nastopoulos, V.; Christou, G.; Tasiopoulos, A. J. *Angew. Chem., Int. Ed.* **2006**, *45*, 7722 and references therein..
(7) Rosi, N. L.; Eckert, J.; Eddaoudi, M.; Vodak, D. T.; Kim, J.; O'Keeffe, M.; Yaghi, O. M. *Science* **2003**, *300*, 1127.
(8) Zheng, S. T.; Wu, T.; Zhang, J.; Chow, M.; Nieto, R. A.; Feng, P. Y.; Bu, X. H. *Angew. Chem., Int. Ed.* **2010**, *49*, 5362.
(9) Hayashi, H.; Cote, A. P.; Furukawa, H.; O'Keeffe, M.; Yaghi, O. M. *Nat. Mater.* **2007**, *6*, 501.
(10) Morris, R. E.; Wheatley, P. S. *Angew. Chem., Int. Ed.* **2008**, *47*, 4966.
(11) Farha, O. K.; Yazaydin, A. O.; Eryazici, I.; Malliakas, C. D.; Hauser, B. G.; Kanatzidis, M. G.; Nguyen, S. T.; Snurr, R. Q.; Hupp, J. T. *Nat. Chem.* **2010**, *2*, 944.
(12) Chen, B. L.; Wang, L. B.; Zapata, F.; Qian, G. D.; Lobkovsky, E. B. *J. Am. Chem. Soc.* **2008**, *130*, 6718.
(13) Tanaka, D.; Kitagawa, S. *Chem. Mater.* **2008**, *20*, 922.
(14) Fang, Q. R.; Zhu, G. S.; Xue, M.; Wang, Z. P.; Sun, J. Y.; Qiu, S. L. *Cryst. Growth Des.* **2008**, *8*, 319.
(15) Fletcher, A. J.; Cussen, E. J.; Bradshaw, D.; Rosseinsky, M. J.; Thomas, K. M. *J. Am. Chem. Soc.* **2004**, *126*, 9750.
(16) Chen, S. C.; Zhang, Z. H.; Zhou, Y. S.; Zhou, W. Y.; Li, Y. Z.; He, M. Y.; Chen, Q.; Du, M. *Cryst. Growth Des.* **2011**, *11*, 4190.
(17) Juan-Alcaniz, J.; Goesten, M.; Martinez-Joaristi, A.; Stavitski, E.; Petukhov, A. V.; Gascon, J.; Kapteijn, F. *Chem. Commun.* **2011**, *47*, 8578.
(18) Pan, Q. H.; Chen, Q. A.; Song, W. C.; Hu, T. L.; Bu, X. H. *CrystEngComm* **2010**, *12*, 4198.
(19) (a) Sun, L. B.; Li, J. R.; Park, J.; Zhou, H. C. *J. Am. Chem. Soc.* **2012**, *134*, 126. (b) Zhang, J.; Bu, J. T.; Chen, S.; Wu, T.; Zheng, S.; Chen, Y.; Nieto, R. A.; Feng, P.; Bu, X. *Angew. Chem., Int. Ed.* **2010**, *49*, 8876.
(20) Panda, T.; Pachfule, P.; Banerjee, R. *Chem. Commun.* **2011**, *47*, 7674.
(21) Wang, D. D.; Peng, J.; Zhang, P. P.; Wang, X.; Zhu, M.; Liu, M. G.; Meng, C. L.; Alimaje, K. *Inorg. Chem. Commun.* **2011**, *14*, 1911.
(22) Zhang, Z. J.; Zhang, L. P.; Wojtas, L.; Nugent, P.; Eddaoudi, M.; Zaworotko, M. J. *J. Am. Chem. Soc.* **2012**, *134*, 924.
(23) (a) Chen, S. M.; Zhang, J.; Wu, T.; Feng, P. Y.; Bu, X. H. *J. Am. Chem. Soc.* **2009**, *131*, 16027. (b) Xu, G.; He, X.; Lv, J.; Zhou, Z.; Du, Z.; Xie, Y. *Cryst. Growth Des.* **2012**, *12*, 3619.
(24) Langley, S. K.; Berry, K. J.; Moubaraki, B.; Murray, K. S. *Dalton Trans.* **2009**, 973.
(25) Foguet-Albiol, D.; Abboud, K. A.; Christou, G. *Chem. Commun.* **2005**, 4282.
(26) Kizas, C. M.; Manos, M. J.; Nastopoulos, V.; Boudalis, A. K.; Sanakis, Y.; Tasiopoulos, A. J. *Dalton Trans.* **2012**, *41*, 1544.
(27) Stamatatos, T. C.; Christou, G. *Inorg. Chem.* **2009**, *48*, 3308.
(28) Wang, W. G.; Zhou, A. J.; Zhang, W. X.; Tong, M. L.; Chen, X. M.; Nakano, M.; Beedle, C. C.; Hendrickson, D. N. *J. Am. Chem. Soc.* **2007**, *129*, 1014.
(29) Tasiopoulos, A. J.; Perlepes, S. P. *Dalton Trans.* **2008**, 5537.
(30) Brechin, E. K. *Chem. Commun.* **2005**, 5141.
(31) Aromi, G.; Brechin, E. K. *Sruct. Bonding (Belin)* **2006**, *122*, 1.
(32) Oxford Diffraction. *CrysAlis CCD and CrysAlis RED*; Oxford Diffraction Ltd: Abingdon, Oxford, England; 2008.
(33) Burla, M. C.; Caliandro, R.; Camalli, M.; Carrozzini, B.; Cascarano, G. L.; De Caro, L.; Giacovazzo, C.; Polidori, G.; Spagna, R. *J. Appl. Crystallogr.* **2005**, *38*, 381.
(34) Sheldrick, G. M. *Acta Crystallogr. A* **2008**, *64*, 112.
(35) Farrugia, L. J. *J. Appl. Crystallogr.* **1999**, 837.
(36) Brandenburg, K. *DIAMOND*, Version 2003.2001d; Crystal Impact GbR: Bonn, Germany; 2006.

(37) (a) Spek, A. L. *J. Appl. Crystallogr.* **2003**, *36*, 7. (b) http://www.topos.ssu.samara.ru/
(38) Xie, L. H.; Liu, S. X.; Gao, B.; Zhang, C. D.; Sun, C. Y.; Li, D. H.; Su, Z. M. *Chem. Commun.* **2005**, 2402.
(39) Macrae, C. F.; Edgington, P. R.; McCabe, P.; Pidcock, E.; Shields, G. P.; Taylor, R.; Towler, M.; van De Streek, J. *J. Appl. Crystallogr.* **2006**, *39*, 453.
(40) Lin, Z. Z.; Jiang, F. L.; Chen, L.; Yue, C. Y.; Yuan, D. Q.; Lan, A. J.; Hong, M. C. *Cryst. Growth Des.* **2007**, *7*, 1712.
(41) Banerjee, D.; Kim, S. J.; Wu, H. H.; Xu, W. Q.; Borkowski, L. A.; Li, J.; Parise, J. B. *Inorg. Chem.* **2011**, *50*, 208.
(42) Liu, D. S.; Huang, G. S.; Huang, C. C.; Huang, X. H.; Chen, J. Z.; You, X. Z. *Cryst. Growth Des.* **2009**, *9*, 5117.
(43) Wang, T. W.; Liu, D. S.; Huang, C. C.; Sui, Y.; Huang, X. H.; Chen, J. Z.; You, X. Z. *Cryst. Growth Des.* **2010**, *10*, 3429.
(44) Arii, H.; Saito, Y.; Funahashi, Y.; Ozawa, T.; Jitsukawa, K.; Masuda, H. *Eur. J. Inorg. Chem.* **2003**, 2917.
(45) Song, X. Q.; Zhou, X. Y.; Liu, W. S.; Dou, W.; Ma, J. X.; Tang, X. L.; Zheng, J. R. *Inorg. Chem.* **2008**, *47*, 11501.
(46) (a) Dybtsev, D. N.; Chun, H.; Kim, K. *Chem. Commun.* **2004**, 1594. (b) Kang, M.; Luo, D.; Luo, X.; Chen, Z.; Lin, Z. *CrystEngComm* **2012**, *14*, 95.
(47) Klunker, J.; Biedermann, M.; Schafer, W.; Hartung, H. *Z. Anorg. Allg. Chem.* **1998**, *624*, 1503.
(48) Calvo-Perez, V.; Shang, M. Y.; Yap, G. P. A.; Rheingold, A. L.; Fehlner, T. P. *Polyhedron* **1999**, *18*, 1869.
(49) Hao, X.-R.; Wang, X. L.; Shao, K.-Z.; Yang, G.-S.; Su, Z.-M.; Yuan, G. *CrysEngComm* **2012**, DOI: 10.1039/C2CE25343G.
(50) Yang, E. C.; Liu, Z. Y.; Wang, X. G.; Batten, S. R.; Zhao, X. J. *CrystEngComm* **2008**, *10*, 1140.
(51) Braverman, M. A.; Supkowski, R. M.; LaDuca, R. L. *J. Solid State Chem.* **2007**, *180*, 1852.
(52) Robl, C. *Z. Anorg. Allg. Chem.* **1988**, *561*, 57.
(53) He, J. H.; Zhang, Y. T.; Pan, Q. H.; Yu, J. H.; Ding, H.; Xu, R. R. *Microporous Mesoporous Mater.* **2006**, *90*, 145.
(54) Shao, K. Z.; Zhao, Y. H.; Lan, Y. Q.; Wang, X. L.; Su, Z. M.; Wang, R. S. *CrystEngComm* **2011**, *13*, 889.
(55) Chen, J. X.; Fan, Q. Y. *Chin. J. Inorg. Chem.* **2011**, *27*, 87.
(56) Zhu, X. H.; Cheng, X. C. *Acta Crystallogr. E* **2011**, *67*, M1641.
(57) Fang, Q. R.; Zhu, G. S.; Xue, M.; Sun, J. Y.; Sun, F. X.; Qiu, S. L. *Inorg. Chem.* **2006**, *45*, 3582.
(58) Wang, Z. Q.; Kravtsov, V. C.; Zaworotko, M. J. *Angew. Chem., Int. Ed.* **2005**, *44*, 2877.
(59) Yu, M.; Liu, S. X. *Chin. J. Struct. Chem.* **2010**, *29*, 353.
(60) Xu, L.; Choi, E. Y.; Kwon, Y. U. *Inorg. Chem.* **2007**, *46*, 10670.
(61) Sun, L.; Qiu, T. R.; Deng, H. *Acta Crystallogr. E* **2011**, *67*, M630.
(62) Jiang, L.; Li, Z. X.; Wang, Y.; Feng, G. D.; Zhao, W. X.; Shao, K. Z.; Sun, C. Y.; Li, L. J.; Su, Z. M. *Inorg. Chem. Commun.* **2011**, *14*, 1077.
(63) Plater, M. J.; Foreman, M. R. S.; Howie, R. A.; Skakle, J. M. S.; Coronado, E.; Gomez-Garcia, C. J.; Gelbrich, T.; Hursthouse, M. B. *Inorg. Chim. Acta* **2001**, *319*, 159.
(64) Shan, W. W.; Xiong, H. L.; Mei, C. Z. *Acta Crystallogr.* **E2011**, *67*, M921.
(65) Majumder, A.; Shit, S.; Choudhury, C. R.; Batten, S. R.; Pilet, G.; Luneau, D.; Daro, N.; Sutter, J. P.; Chattopadhyay, N.; Mitra, S. *Inorg. Chim. Acta* **2005**, *358*, 3855.
(66) Che, G. B.; Liu, C. B.; Liu, B.; Wang, Q. W.; Xu, Z. L. *CrystEngComm* **2008**, *10*, 184.
(67) Xu, L.; Choi, E. Y.; Kwon, Y. U. *Inorg. Chem. Commun.* **2008**, *11*, 150.
(68) Davies, K.; Bourne, S. A.; Ohrstrom, L.; Oliver, C. L. *Dalton Trans.* **2010**, *39*, 2869.
(69) Yaghi, O. M.; Davis, C. E.; Li, G. M.; Li, H. L. *J. Am. Chem. Soc.* **1997**, *119*, 2861.
(70) (a) Li, X. J.; Sun, D. F.; Cao, R.; Sun, Y. Q.; Wang, Y. Q.; Bi, W. H.; Gao, S. Y.; Hong, M. C. *Inorg. Chem. Commun.* **2003**, *6*, 908. (b) Lu, J.; Mondal, A.; Moulton, B.; Zaworotko, M. J. *Angew. Chem., Int. Ed.* **2001**, *41*, 2113.
(71) Shi, Z.; Li, G. H.; Wang, L.; Gao, L.; Chen, X. B.; Hua, J.; Feng, S. H. *Cryst. Growth Des.* **2004**, *4*, 25.
(72) Xu, L.; Choi, E. Y.; Kwon, Y. U. *Inorg. Chem. Commun.* **2008**, *11*, 1190.
(73) Kim, J.; Chen, B. L.; Reineke, T. M.; Li, H. L.; Eddaoudi, M.; Moler, D. B.; O'Keeffe, M.; Yaghi, O. M. *J. Am. Chem. Soc.* **2001**, *123*, 8239.
(74) Fu, Y.; Li, G. B.; Liao, F. H.; Xiong, M.; Lin, J. H. *J. Mol. Struct.* **2011**, *1004*, 252.
(75) Li, X. J.; Cao, R.; Sun, D. F.; Yuan, D. Q.; Bi, W. H.; Li, X.; Wang, Y. Q. *J. Mol. Struct.* **2004**, *694*, 205.
(76) Wang, B. C.; Wu, Q. R.; Hu, H. M.; Chen, X. L.; Yang, Z. H.; Shangguan, Y. Q.; Yang, M. L.; Xue, G. L. *CrystEngComm* **2010**, *12*, 485.